Volume 16 Number 17 1988 Nucleic Acids Research

An elongated model of the *Xenopus laevis* transcription factor IIIA-5S ribosomal RNA complex derived from neutron scattering and hydrodynamic measurements

Peter A.Timmins*, Jörg Langowski[1] and Raymond S.Brown[2]+

Institut Laue-Langevin, 156X, 38042 Grenoble Cedex, [1]EMBL Outstation, c/o ILL, 156X, 38042 Grenoble Cedex, France and [2]EMBL, Postfach 102209, Meyerhofstrasse 1, D-6900 Heidelberg, FRG

Received July 8, 1988; Accepted August 5, 1988

Abstract

The precise molecular composition of the *Xenopus laevis* TFIIIA-5S ribosomal RNA complex (7S particle) has been established from small angle neutron and dynamic light scattering. The molecular weight of the particle was found to be 95700±10000 and 86700±9000 daltons from these two methods respectively. The observed match point of 54.4% D_2O obtained from contrast variation experiments indicates a 1:1 molar ratio. It is concluded that only a single molecule of TFIIIA, a zinc-finger protein, and of 5S RNA are present in this complex. At high neutron scattering contrast a radius of gyration of 42.3±2 Å was found for the 7S particle. In addition a diffusion coefficient of $4.4 \cdot 10^{-11}$ [$m^2 s^{-1}$] and a sedimentation coefficient of 6.2S were determined. The hydrodynamic radius obtained for the 7S particle is 48±5 Å. A simple elongated cylindrical model with dimensions of 140 Å length and 59 Å diameter is compatible with the neutron results. A globular model can be excluded by the shallow nature of the neutron scattering curves. It is proposed that the observed difference of 15 Å in length between the 7S particle and isolated 5S RNA most likely indicates that part(s) of the protein protrudes from the end(s) of the RNA molecule. There is no biochemical evidence for any gross alteration in 5S RNA conformation upon binding to TFIIIA [1].

Introduction

A stable complex of TFIIIA associated with 5S RNA (7S particle) is found in abundance in the previtellogenic oocytes of *Xenopus laevis*[2,3]. In this way 5S RNA is stored prior to the onset of ribosome biosynthesis and assembly in the developing oocyte. In addition TFIIIA plays a role in the regulation of oocyte 5S RNA gene expression binding to approximately 50 base-pairs of the internal control region (reviewed in [4]).

TFIIIA has been identified as a zinc-finger protein [5-7] containing nine potential RNA/DNA-binding domains. The polypeptide chain in each of these domains is folded about a structural zinc ion coordinated to invariant pairs of histidines and of cysteines [8,9]. A compact folded structure is predicted for a single zinc finger [5,7,10]. Evidence for the existence of this type of structure is provided by the difficulty of several proteases to cut within the zinc finger domains of TFIIIA [6,11].

A physico-chemical study of isolated TFIIIA [12] shows that the protein may be elongated with dimensions 135×18 Å and appears to exist as a monomer in solution. An extended conformation has also been proposed for 5S RNA which is the other component of the 7S particle. X-ray and dynamic light scattering measurements of rat liver 5S RNA are

compatible with a Y-shaped model [13] of maximum length 109 Å and a thickness of 16 Å. To date the only neutron investigation that has been reported is a small angle scattering study of *E. coli* 5S RNA and its complexes with ribosomal proteins L5, L18 and L25 [14].

The extent of protein-RNA interactions in the native 7S particle has been revealed using biochemical and chemical probes [1,and refs. therein]. However, any plausible model requires the exact molecular composition of the complex to be known. A Stokes radius of 47 Å obtained by gel column chromatography [R. S. B., unpublished results], which corresponds to the elution behaviour of a globular protein of 175000 daltons is consistent with there being two molecules of each component present. If there are in fact only one of each in the 7S particle then the Stokes radius value indicates an extremely asymmetric shape. Both of these possibilities are in agreement with the RNA/protein ratio in the 7S particle which has been determined to be 1:1 [2]. Similar models for the binding of TFIIIA to the 5S RNA gene internal control region have been proposed [15] where a single protein molecule interacts in an extended fashion along the DNA.

An absolute determination of the molecular weight [16] can be made from neutron small angle scattering measurements. This value will unequivocally establish the molecular composition of the 7S particle. Confirmation of this result is provided from measurements of hydrodynamic properties using dynamic light scattering and sedimentation analysis.

The technique of contrast variation in H_2O/D_2O mixtures [17] is particularly applicable to RNA/protein complexes such as the 7S particle and provides a means to investigate the internal organisation of the components within the 7S particle.

In the present work the main purpose of undertaking a physical characterization of the 7S particle is to establish the exact number of TFIIIA and oocyte-type 5S RNA molecules in the complex. Such knowledge facilitates both construction and evaluation of models of zinc finger-RNA interactions in the 7S particle [1]. Furthermore, information gained about the shape, dimensions and molecular composition of the 7S particle are of assistance in its crystallographic structure analysis [18].

Materials and Methods

Preparation of 5S RNA

Oocyte-type 5S RNA was isolated from 42S particles that were prepared from the ovaries of immature female *X. laevis* as described in [19]. The 42S particles in 100 mM NaCl, 2.5 mM $MgCl_2$ and 50 mM Tris-HCl, pH 8.5 (buffer A) were extracted three times with 2 volumes of water-saturated phenol/chloroform (1:1 v/v) at 0 °C. 5S RNA and tRNA were recovered by precipitation with two volumes of ethanol at -20 °C in the presence of 200 mM sodium acetate. After centrifugation the pellet was resuspended in 2 ml of buffer A, filtered through a Millex HA unit, 0.45 μm (Millipore) and applied to an Ultragel ACA54 (LKB) column (2.6×100 cm) at 10 ml per hour. The leading peak of 5S RNA was pooled and recovered by ethanol precipitation.

Denaturing 12.5% PAGE reveals the presence of a slower moving minor component ca. 25% (as judged by ethidium bromide staining). This effect is attributed to the presence of

either one (minor species) or three phosphates (major species) at the 5' terminus of 5S RNA rather than variable sequence extension at the 3' end [1].

5S RNA was renatured by heating to 56 °C for 10 min followed by slow cooling in 100 mM NaCl, 2.5 mM $MgCl_2$ and 20 mM Tris-HCl, pH 8.0 (buffer B) and dialyzed extensively at 10 °C. The concentration of 5S RNA was determined using an extinction coefficient of 20.5±0.4 absorbance units per mg at 260 nm. This factor was determined using the colorimetric acid-molybdate method described in [20] to measure the amount of inorganic phosphate released upon ashing 5S RNA.

Purification of 7S Particles

The 7S particles were prepared by the method described in [1]. The TFIIIA in the sample was at least 90% pure from SDS-PAGE analysis using Coomassie Brilliant blue stain. Prior to scattering experiments samples were extensively dialyzed at 10 °C against 100 mM NaCl, 1 mM dithiothreitol and 20 mM Tris-HCl, pH 8.0 (buffer C) and filtered through Millex HV4 units (Millipore) to remove aggregates and dust. The concentration of the 7S particles was taken to be twice (based on a weight ratio of 1:1 for the complex [2]) that of the incorporated 5S RNA using a conversion factor of 22.6±0.9 absorbance units per mg of 5S RNA at 260 nm. Sample concentrations were typically 2-5 mg/ml.

Neutron Scattering

Data collection. Neutron small angle scattering spectra were measured on the D11 instrument [21] or the D17 instrument at the high flux reactor of the Institut Laue-Langevin, Grenoble. Spectra were measured using an incident neutron wavelength [λ] of 10 Å ($\Delta\lambda/\lambda$=8%) and sample to detector distances of 5.0 and 2.0 m giving **Q**-ranges ($Q=4\pi\sin\theta/\lambda$; 2θ=scattering angle) of 0.006 to 0.044 and 0.014 to 0.11 [$Å^{-1}$] respectively. For the 80% D_2O 7S particle and the 5S RNA data were measured on the instrument D17 which is very similar to D11. Here the sample to detector distance was fixed at 2.91 m and the wavelength used was 11.0 Å ($\Delta\lambda/\lambda$=10%) corresponding to a **Q**-range of 0.01 to 0.08 [$Å^{-1}$]. The samples were contained in rectangular quartz cells (Hellma, France) having path lengths of 1 mm (for 0% and 20% D_2O) or 2 mm (for 80% and 100% D_2O). Samples were prepared by dialysis at 10 °C against the appropriate D_2O/H_2O containing buffer for 12-16 h with two changes of buffer. Equilibration of H/D exchange between buffer and sample was checked by verifying that their neutron transmissions were identical. All measurements were carried out at 10 °C. Each series of neutron scattering measurements consisted of sample, buffer, a 1 mm thick foil of cadmium (which occludes the beam and is a measure of the electronic noise of the detector as well as of extraneous neutrons), empty cell and water. The latter corrects for non-uniform sensitivity of the two-dimensional detector and also serves to put the data on an absolute scale. Precise D_2O contents were determined by neutron transmission measurements.

The data from the two-dimensional detector were circularly averaged using standard programs [22] and each sample corrected for buffer scattering and normalised to the scattering of water, yielding a series of curves expressed as ln I(**Q**) versus **Q**.

Data analysis. The data measured over the two **Q**-ranges on D11 (corresponding to 2 or 5 m sample-detector distance) were subject to different interpretations. The 5 m data were

plotted as ln I(Q) versus Q^2 (Guinier plot) from which were obtained the radii of gyration R_g, and intensity at zero angle I(0) [23]. Only a single instrumental configuration was used on D17.

The D_2O mole fraction at which the zero angle scattering falls to zero (isopycnic point) was obtained from a plot of $\sqrt{[I(0)/c]}$ (normalized to unit thickness and transmission) *versus* D_2O mole fraction in the solvent.

The molecular weight was calculated by the method of Jacrot and Zaccai [16] from the value of the zero angle scattering in H_2O using the expression:

$$\frac{I(0)}{c} = \frac{4\pi T_s}{1-T_w} N_a \cdot t \cdot M \cdot 10^{-3} \cdot \left\{ \frac{\Sigma b}{M} - \frac{\rho_s V}{M} \right\}^2 \quad (1)$$

where:

I(0)	= the scattered intensity at Q=0
c	= concentration in mg/ml
T_s	= Neutron transmission of the sample
T_w	= Neutron transmission of H_2O
N_A	= Avogadro's number
t	= path length of the neutron beam (in cm)
M	= molecular weight
$\Sigma b/M$	= sum of the neutron scattering lengths per unit molecular weight of the particle
ρ_s	= scattering length density of the solvent
V	= particle volume

The value of $\Sigma b/M$, $2.714 \cdot 10^{-14}$ [cm dalton^{-1}], was calculated from the known amino acid composition of the protein, the nucleotide content of *X. laevis* 5S RNA and a relative stoichiometry of protein to RNA of 1:1 as obtained from the isopycnic point.

The 2 m data extended the observable Q-range by a factor of 2.5 and was used to fit simple cylindrical models. This was carried out using the program CYLFIT written by S. Cusack (EMBL, Grenoble), where the experimental scattering curve is fitted by a cylindrical shell model described by a number of parameters, shell radius and scattering length density of each shell, convoluted with the instrumental smearing parameters (wavelength spread, beam divergence). Owing to the rather limited extent of the data ($.014 < |Q| < .11$) models consisting of only a single shell of variable diameter were considered. For the same reason no attempt was made to compare with detailed models via the Debye [24] formula.

Dynamic Light Scattering

Diffusion coefficients of the 7S particle and isolated 5S RNA were determined using dynamic light scattering. Intensity correlation functions $G^{(2)}(\tau)$ were collected on an instrument consisting of an AMTEC goniometer, Malvern K7023 correlator and a Spectra-Physics 165 argon ion laser operating at 400 mW on the 488 nm line. The measuring cell was a 1 cm diameter quartz cuvette suspended in an 8 cm diameter decahydronaphthalene

index matching bath. The set-up allows us to collect accurate data from sample volumes as small as 300 µl.

Data collection was carried out using a software "dust filter" which collects data at short intervals, accumulating only those portions whose scattering density is below a given threshold. Thus dust "tyndalls" that can remain even after careful filtering are very effectively avoided. For each measurement we accumulated 200 to 300 autocorrelation functions of 2 secs duration fulfilling the dust elimination criteria.

Multiexponential fitting of the data was performed using either the DISCRETE program developed by Provencher [25] on the first order correlation function $G^{(1)}(\tau)$ or a fitting routine developed by us that fits directly the second order correlation function to a squared sum of exponentials. Both methods gave comparable results.

Experiments were performed in buffer B (5S RNA) and buffer C (7S particle). Diffusion coefficients were temperature- and viscosity-corrected to water at 20 °C. Buffer viscosities were measured in an automated capillary viscosimeter (Schott, Mainz, FRG). All solutions were filtered directly into the measuring cell through 0.1 µm Nucleopore polycarbonate membrane filters (Nucleopore, Tübingen, FRG) to remove dust or any large aggregates.

Analytical Centrifugation

Sedimentation runs were performed in a MSE Centriscan analytical ultracentrifuge equipped with a UV scanner. Absorption was monitored at 254 nm. The runs were performed at 20 °C at angular velocities of 50000 or 60000 rpm. Sedimentation coefficients were obtained from linear regression lines where ln r was plotted against sedimentation time, r being the distance from the center of the rotor to the sedimenting boundary. The S-values were corrected to $s^0_{20,w}$.

Results

Neutron Scattering

Neutron scattering curves were measured for the 7S particle in (nominally) 0, 20, 80 and 100% D_2O as well as for 5S RNA in H_2O. The precise D_2O contents are given in Table 1. The lower angle data plotted as Guinier curves (ln I(Q) *versus* Q^2) are shown in Figure 1.

It can be seen from these curves that the radii of gyration vary rather little with contrast but, on the other hand, the R_g for the 7S particle is considerably larger than that for 5S RNA. Indeed for the 7S particle the radius of gyration at high contrast (H_2O or D_2O) is around 42.3±2 Å compared with 32.4±3 Å for the 5S RNA in H_2O (Table 1). The molecular weight obtained from I(0) in H_2O is 95700±10000, the error being estimated from the statistical error in I(0) as well as the uncertainty in concentration arising from both the error in the extinction coefficient and the presence of small amounts of higher stoichiometry particles. The latter are estimated from non-denaturing PAGE to comprise about 5% of the material. Fig. 2 shows a plot of $\sqrt{[I(0)/c]}$ versus % D_2O for the complex and indicates a match point at 54.4% D_2O, showing that the particle is indeed an equimolar complex of TFIIIA and 5S RNA. The match points calculated for 2:1, 1:1 and 1:2 (protein/RNA) are respectively 49.2%, 53.7% and 58.5% D_2O. This result combined with the observed molecular weight confirms that the particle is in fact a 1:1 complex.

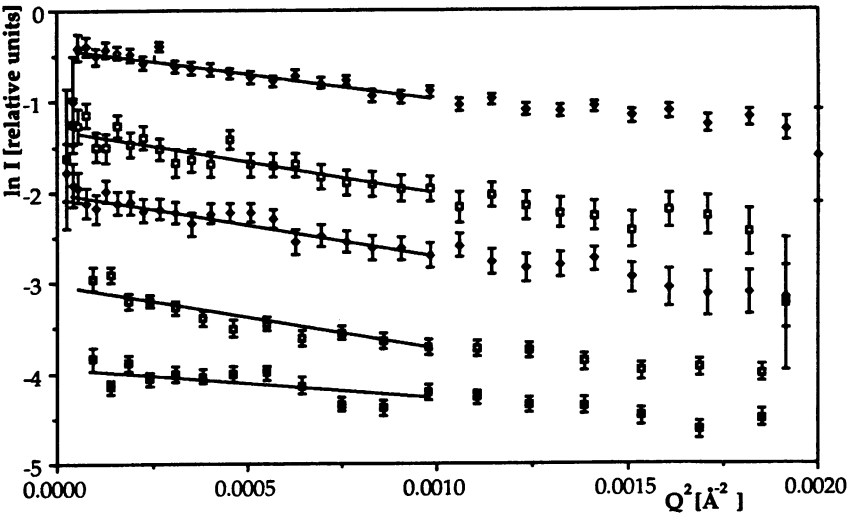

Fig.1: Small angle scattering curves (Guinier plots) of the 7S particle in 100%, 0%, 20%, and 80% D_2O (from top to bottom), and 5S RNA (lower curve). Intensities were scaled by arbitrary amounts to separate the curves.

The most obvious qualitative conclusion to be drawn from the radius of gyration measurements is that the 7S particle and the isolated RNA are somewhat elongated objects. A globular protein of molecular weight 80000 for example would have a radius of gyration of only 22 Å or conversely, a 45 Å radius of gyration would indicate a globular molecule of molecular weight $\approx 6 \cdot 10^5$. The elongated shape is also reflected in the weakness of the

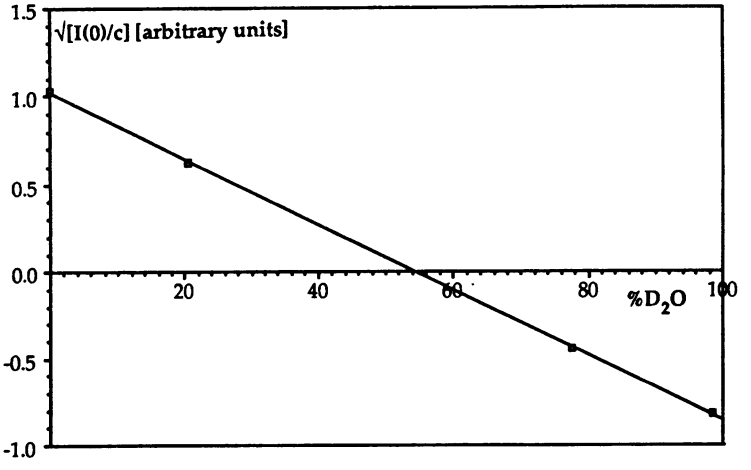

Fig.2: Determination of the match point for the 7S particle from a plot of $\sqrt{[I(0)/c]}$ versus % D_2O.

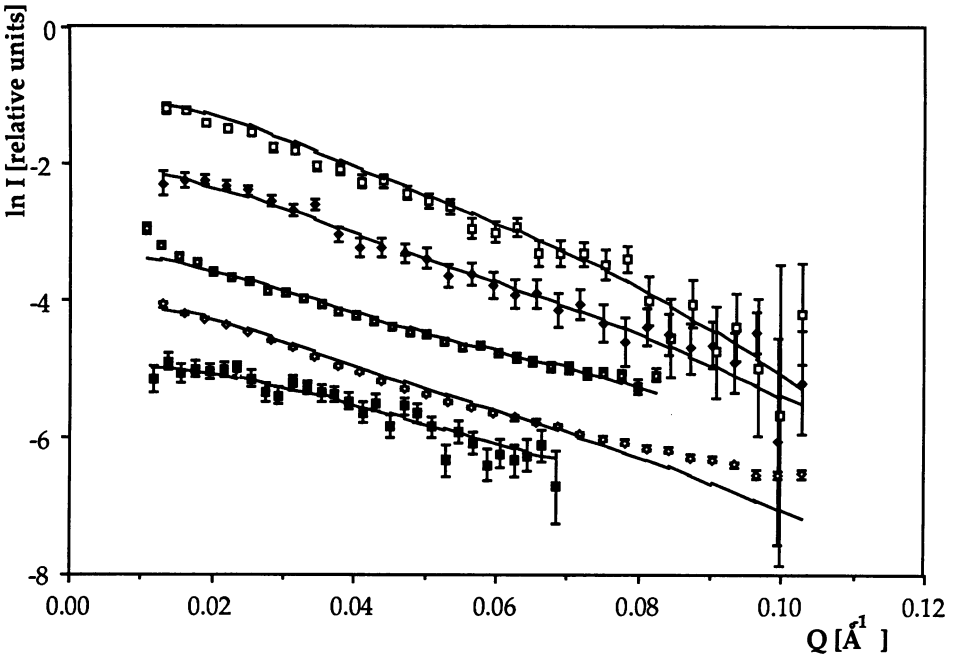

Fig.3: Fit of cylindrical models to the small angle scattering curves; from top to bottom: 7S particle at 0%, 20%, 80%, and 100% D_2O and 5S RNA at 0% D_2O. The curves were scaled by arbitrary factors to separate them.

scattering compared with that from a globular particle of the same radius of gyration. This meant that we were unable to obtain data of sufficient precision at low contrast in the Guinier range to determine precisely the relative dispositions of the protein and RNA about the particles' centre of scattering mass. Moreover the radii of gyration of such particles are dominated by the longest dimension and therefore contain very little information on any lateral separation of scattering mass.

We therefore measured, for the same samples, the scattering curves at higher angles (detector at 2 m). The radii of gyration measurements suggested that the structure was elongated and, as small angle scattering can never produce an unique model, we decided to interpret these higher angle data by imposing a cylindrical model and investigating its variation with contrast.

The best models obtained, fitted to the four different contrast data sets of 7S particle and of the 5S RNA, are shown in Fig. 3. The parameters used to fit these curves (cylinder length, L and radius R) are shown in Table 1. It can be seen that all the 7S particle curves can be fitted by cylinders of the same length but different radii whereas the 5S RNA data is best described by a much shorter (length=115 Å) rod. The fitting is in fact rather insensitive to the actual length, and reasonable fits could be found for values between 135 and 160 Å. A

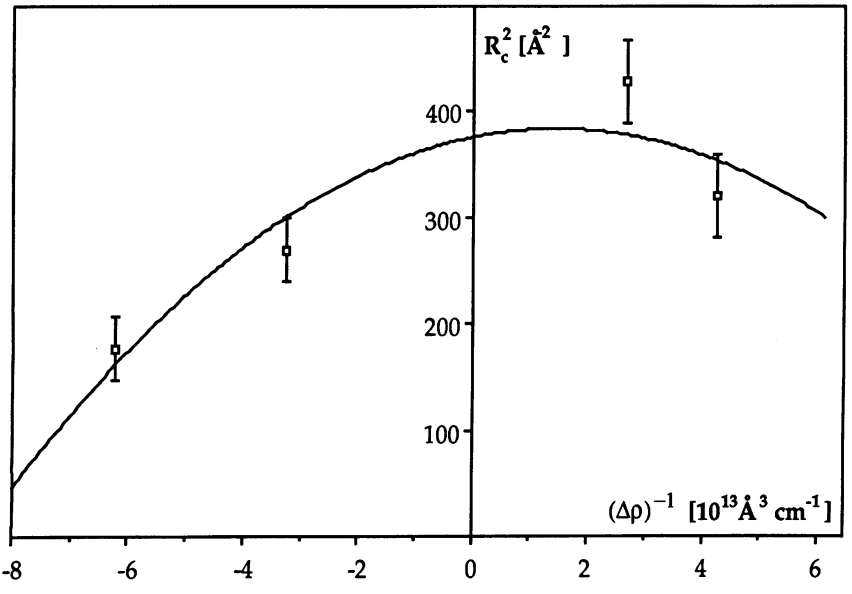

Fig. 4: Variation of cross-sectional radius of gyration with contrast (Stuhrmann plot) for the 7S particle.

fixed value of 140 Å was chosen to remain consistent with the lower angle (Guinier range) data.

The different radii obtained from the model fits, in fact reflect a difference in the radial distribution of scattering density within the molecule. This may also be described as a cross-sectional radius of gyration, R_c. The R_c obtained in this way is plotted as a function of the inverse contrast (Stuhrmann plot [26]) in Fig.4. These data may be satisfactorily fitted by a parabola as shown, indicating that the centres of scattering density of the two components, RNA and protein, are probably at different radial locations. The cross-sectional radii of gyration are also listed in Table 1.

Table 1: Neutron Scattering Parameters for 5S RNA and the 7S particle.

		R_g [Å]	Mol.wt.	L [Å]	R [Å]	R_c [Å]
7S particle	0%D_2O	42.3±2	95700± 10000	140	29.3	20.7
	20.5%D_2O	41.8±2	-	140	25.4	17.9
	77.5%D_2O	37.5±5	-	140	18.8	13.3
	98.5%D_2O	42.3±2	-	140	23.3	16.4
5S RNA	0% D_2O	36±3	n.d.	115	19.1	13.5

Hydrodynamic Measurements

The sedimentation and diffusion coefficients of the 7S particle and isolated 5S RNA are shown in Table 2. Within the limits of error we could not detect any difference between a sample containing 2.5 mM Mg^{2+} and two Mg-free samples of both the 7S particle and 5S RNA. The values given are the average of three measurements, the error being ±8% on the diffusion coefficient and ±2% on the S-value. This gives a total error in molecular weight of ±10%.

The hydrodynamic radius was calculated from the Stokes/Einstein relationship $R_s = k_B T/6\pi\eta D$, where D is the diffusion coefficient, k_B Boltzmann's constant and η the viscosity of the medium. From these data the shapes of the 7S particle and of the 5S RNA can be described as cylinders with certain axial ratios. The axial ratio was calculated in two different ways. First, we may use the R_g from neutron scattering together with the hydrodynamic radius R_s. For a rod of half length a and radius b,

$$R_g^2 = \frac{a^2}{3} + \frac{b^2}{2} \quad (2) \qquad \text{and} \qquad R_s = \frac{a}{\ln\left(\frac{a}{b} + \gamma\right)} \quad (3)$$

where γ is approx. 0.5 for the range of axial ratios considered here [27]. From these relationships, R_g/R_s will give us the axial ratio a/b.

On the other hand we may use the sedimentation data, the partial specific volume of the particle and the known molecular weight (from the sequence) to calculate the hydrodynamic radius R_s from eq. (3), and from that quantity the axial ratio of an equivalent cylinder independently of the neutron scattering data. Both values are in good agreement (Table 2). Typical cylindrical shapes in agreement with the hydrodynamic data would be:

7S particle: length 140 Å, diameter 60 Å, with a theoretical diffusion coefficient $D = 4.35 \cdot 10^{-11}$ [$m^2 s^{-1}$]
5S RNA: length 128 Å, diameter 32 Å, with $D = 6.2 \cdot 10^{-11}$ [$m^2 s^{-1}$]

Molecular weights were also calculated from S and D, assuming partial specific volumes of v = 0.72 [$cm^3 g^{-1}$] for TFIIIA [28] and 0.53 [$cm^3 g^{-1}$] for RNA [16]. The partial specific volume of the 7S particle was taken as 0.61 [$cm^3 g^{-1}$] on the basis of the known 1:1 molar ratio [2] confirmed by the neutron match point, and we assumed that no volume changes occurred upon complex formation.

Table 2: Hydrodynamic parameters of 5S RNA and the 7S particle.

	$D_{20,w}$ [$m^2 s^{-1}$]	$s^0_{20,w}$ [S]	R_s [nm]	Mol.wt. (from s/D)	Mol.wt. (theor.)	axial ratio of cylinder from R_s/R_g	from s and M_{theor}
5S RNA	$6.2 \cdot 10^{-11}$	4.6	3.5	42030	41560	3.7	4.0
7S particle	$4.4 \cdot 10^{-11}$	6.2	4.8	86700	81893	2.5	3.0

The measured molecular weights for both the 7S particle and 5S RNA are in agreement with the theoretical values calculated from their sequences and including Na^+ as the RNA counterion.

Conclusion and Discussion

Both the neutron scattering and the hydrodynamic results presented here indicate that the 7S particle is highly elongated and is a 1:1 complex of TFIIIA and 5S RNA. Moreover it is clear that 5S RNA is itself elongated but less so than the 7S particle. This would suggest that not all of the TFIIIA molecule is bound to 5S RNA and that some 15 Å length of protein protrudes from one or both ends of the RNA. Indeed the non-zinc-finger C-terminal region of TFIIIA, which is easily removed by protease digestion, is unlikely to be bound to 5S RNA.

The techniques we have utilised do not permit us to derive unique models. However the proposal of simple rod-like models (Fig. 5) for the 7S particle and 5S RNA are entirely consistent with the experimental data. The neutron contrast variation data do not allow us to propose more detailed models, but clearly demonstrate the existence of very elongated particles. This means that different regions of the scattering curves are dominated by particular features of the model. The Guinier range indicates mainly the length of the particles whilst the higher angle scattering is dominated by their radial dimension. Thus the rather small observed variation with contrast of the R_g indicates that at most contrasts the 7S particle appears as an object of approximately the same length. The data at 80% D_2O are perhaps the only ones to indicate a smaller dimension (Rg=37±5 Å, L≈140 Å); in this D_2O/

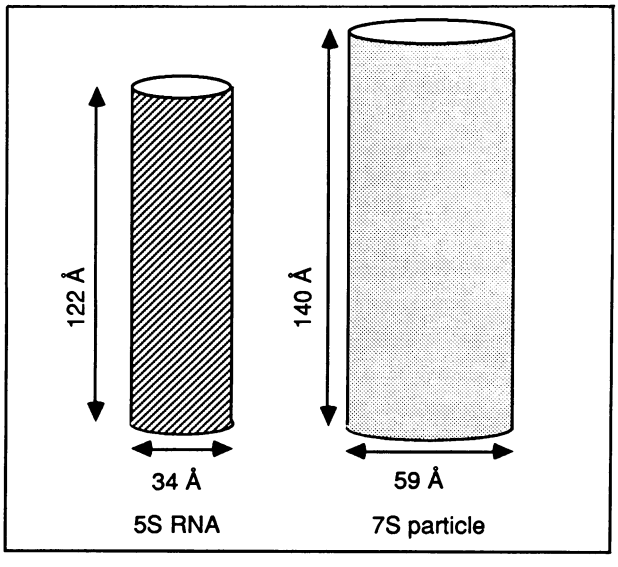

Fig.5: Dimensions of proposed models for the 7S particle and 5S RNA (averaged from neutron and hydrodynamic data).

H_2O mixture the RNA would have very low contrast and the scattering would be dominated by the length of the protein.

The higher angle data contain mainly information on the radial dimensions of the elongated particle. In H_2O where both protein and RNA have rather high contrast we obtain the largest radial dimension whereas at low contrast, both negative and positive, the apparent radius is rather smaller. This suggests that the TFIIIA and RNA interact in a complex manner that cannot be described adequately by two rods simply associated side-by-side nor with one component completely surrounding the other.

ACKNOWLEDGEMENTS

We would like to thank Adrian Kingswell for skillful technical assistance and Dr. Bernard Jacrot for encouragement of this work.

*To whom correspondence should be addressed

+Present address: Department of Microbiology and Molecular Genetics, Harvard Medical School and Howard Hughes Medical Institute, Harvard University, 7 Divinity Avenue, Cambridge, MA 02138, USA

REFERENCES

1. Christiansen, J., Brown, R.S., Sproat, B.S. and Garrett, R.A. (1987) EMBO J. **6**, 453-460.
2. Picard, B. and Wegnez, M. (1979) Proc. Natl. Acad. Sci. U.S.A. **76**, 241-245
3. Pelham, H.R.B. and Brown, D.D. (1980) Proc. Natl. Acad. Sci. U.S.A. **77**, 4170-4174.
4. Brown, D.D. (1984) Cell **37**, 359-365
5. Brown, R.S., Sander, C. and Argos, P. (1985) FEBS Lett. **186**, 271-274.
6. Miller, J., McLachlan, A.D. and Klug, A. (1985) EMBO J. **4**,1609-1614.
7. Brown, R.S. and Argos, P. (1986) Nature **324**, 215.
8. Diakun, G.P., Fairall, L. and Klug, A. (1986) Nature **324**, 698-699.
9. Frankel, A.D., Berg, J.M. and Pabo, C.O. (1987) Proc. Natl. Acad. Sci. U.S.A. **84**, 4841-4845
10. Berg, J.M. (1988) Proc. Nat. Acad. Sci. USA **85**, 99-102.
11. Smith, D.R., Jackson, I.J. and Brown, D.D. (1984) Cell **37**, 645-652.
12. Bieker, J.J. and Roeder, R.G. (1984) J. Biol. Chem. **259**, 6158-6164.
13. Muller, J.J., Zalkova, T.N., Zirwer, D. Misselwitz, R.,Gast, K. Serdyuk, I.N., Welfle, H. and Damaschun, G. (1986) Eur. Biophys. J. **13**, 301-307.
14. Lorentz, S., Erdmann, V. A., May, R., Stockel, P., Strell, I. and Hoppe, W. (1980) Eur. J. Cell Biol. **22**, M 396, 134.
15. Fairall, L., Rhodes, D. and Klug, A. (1986) J. Mol. Biol., **192**, 577-591.
16. Jacrot, B. and Zaccai, G. (1981) Biopolymers **20**, 2413-2426.
17. Timmins, P.A. and Zaccai, G. (1988) Eur. Biophys. J. **15**, 257-268
18. Brown, R.S., Ferguson, C., Kingswell, A., Winkler, F.K. and Leonard, K.R. (1988) Proc. Nat. Acad. Sci. USA **85**, 3802-3804.
19. Mattaj, I.W., Coppard, N.J., Brown, R.S., Clark, B.F.C. and De Robertis, E.M. (1987) EMBO J. **6**, 2409-2413.
20. Ames, B.N., in: *Methods in Enzymology* (eds. Neufeld, E.F. and Ginsburg, V.), vol. 8, pp.115-118, Academic Press, New York and London.
21. Ibel, K. (1976) J. Appl. Cryst. **9**, 296-309

22. Ghosh. (1981) ILL Internal Report 81GH29T
23. Guinier, A. and Fournet, G., *Small Angle Scattering by X-rays*, Wiley, New York 1955.
24. Debye, P. (1915) Ann. Phys. (Leipzig) **46**, 2927-2929
25. Provencher, S.W., (1976) Biophys. J. **16**, 27
26. Ibel, K. and Stuhrmann, H. (1975) J. Mol. Biol. **93**, 255-265
27. Tirado, M.M. and Garcia de la Torre, J., (1979) J. Chem. Phys. **71**, 2581
28. Zamyatnin, A.A. (1972) Prog. Biophys. Mol. Biol. **24**, 109-123.